THE ASTROPHYSICAL JOURNAL, 469:131–137, 1996 September 20

STAR FORMATION IN THE OUTER RESONANCE RING OF NGC 1300

DEBRA MELOY ELMEGREEN,[1] BRUCE G. ELMEGREEN,[2] FREDERICK R. CHROMEY,[1] AND DAVID ALAN HASSELBACHER[1]

Received 1995 August 7; accepted 1996 April 16

ABSTRACT

Surface photometry of the barred galaxy NGC 1300 in B and I bands reveals an outer pseudo-ring with star formation knots located at the positions of 10^8 $M_\odot$ H I clouds previously mapped by M. England with the VLA. The age of the ring from the $B-I$ colors is estimated to be $\sim 10^9$ yr, and the age of the star formation knots is estimated to be $\sim 2 \times 10^7$ yr. Stability considerations suggest that the H I clouds formed by gravitational condensation along the ring periphery. If the outer extent of the ring is at the outer Lindblad resonance, then the bar ends slightly outside the inner 4:1 resonance and corotation is at the position of the break and dust lane crossing midway out in the spiral arms.

Subject headings: galaxies: individual (NGC 1300) — galaxies: kinematics and dynamics — galaxies: photometry — galaxies: spiral — galaxies: structure — stars: formation

1. INTRODUCTION

NGC 1300 is a barred galaxy with a Hubble type SB(rs)bc (de Vaucouleurs et al. 1991, hereafter RC3). Two nearly symmetric spiral arms wrap into an outer ring that resembles an open figure-8, with a long axis offset 70° from the bar. The ring in NGC 1300 was not apparent in early classifications; for example, the galaxy is listed as having an inner ring but no outer ring in the catalog by de Vaucouleurs & Buta (1980). Near-infrared photometry by Baumgart & Peterson (1986) does not show the ring either, but Buta & Crocker (1993) and Buta (1995) note its presence on the SRC-J survey prints; they list it as type R', intermediate between types R'_1 and R'_2 as described in Buta & Crocker (1991). The northern part of the outer ring is also evident on the Palomar Observatory Sky Survey print, and on the CD-ROM Digitized Sky Survey. According to Buta and Crocker, features like this should be termed pseudo-rings, rather than true rings, because they do not close completely; in this paper we simply call it a ring, using the generic sense of the term.

Test particle simulations of barred galaxies in Schwarz (1981) and Byrd et al. (1994) suggest that outer rings and pseudo-rings are located near the outer Lindblad resonance (OLR; Buta & Crocker 1991, 1993). The R'_1 pseudo-rings are aligned with long axes perpendicular to the bar, ending at about the OLR. The R' ring in NGC 1300 is similar to this, except for the 20° offset of the major axis from the perpendicular to the bar, and is therefore a candidate for an OLR ring. If the OLR is at the major axis of the ring, then the bar ends between the inner 4:1 and corotation resonances, according to the flat rotation curve in England (1989a). These results are discussed further in § 3.1.

Here we present calibrated B and I band surface photometry of NGC 1300 in order to estimate the age of the outer ring and several of the star formation features that reside in the ring (§ 3.2). We find that the ring is bluer than the adjacent disk at larger and smaller radii, which is typical for outer rings (Buta & Crocker 1991), and that it contains even bluer star formation clumps at the locations of giant H I clouds found by England (1989b). The H I data is used to evaluate the Toomre stability parameter Q in the ring. On the basis of these data, we suggest that the ring formed over 10^9 yr ago by the torquing action of the bar, which must have formed earlier. Star formation in the ring apparently began when the accumulated gas at the OLR reached the threshold column density $\sim 10^9$ yr ago, and it continues in the ring today at a low level, with large faint patches 10^7–10^8 yr old.

2. OBSERVATIONS AND RESULTS

NGC 1300 was observed with the KPNO Burrell Schmidt 0.6 m telescope in B and I bands on 1994 January 3–7 and 1995 October 26-27, using the s2ka chip with 2048 × 2048 pixels and 2.″0 pixel^{-1} scale. Eleven exposures in B totaling 9400 s and 13 exposures in I totaling 10,600 s were obtained. Several 100 s exposures in I were also obtained to correct for saturation of the nucleus of the galaxy on the deeper frames. The telescope pointing was dithered between exposures to correct for bad columns and permit construction of dark sky flats.

The images were bias-subtracted and flattened, then combined and sky-subtracted in the usual way using the Image Reduction and Analysis Facility (IRAF) program. Twilight sky flats from the whole run were averaged to minimize the noise, and the heavily smoothed dark-sky flats applied as an illumination correction.

Figure 1 shows the resulting B and I images plotted as log of the intensity (north is up). The calibration bar on the lower right is R_{25}, and on the lower left it is 100 pixels (3.′38). The faint ring in the outer regions is seen as a broad plateau and an extension of the two main arms; it is not completely symmetric because it is wider and brighter in the north. The outer arms curve inward and close to resemble a figure-8, although they do not quite wind 180° with respect to the ends of the bar.

Figure 2 shows radial profiles of relative surface brightness parallel and perpendicular to the bar in B and I bands, and the radial surface brightness profiles of calibrated $B-I$ color uncorrected for extinction. The distance on the abscissa is not deprojected to correct for the inclination of the galaxy in the sky. The ends of the bar are indicated by the symbol "b," spiral arms are indicated by "s," and the outer ring is indicated by "r." The difference between "r" and "s" is subjective: we consider the ring to be the outer part of the spiral arm on and beyond the minor axis. The ring is more

[1] Vassar College Observatory, Poughkeepsie, NY 12601.
[2] IBM Research Division, T. J. Watson Research Center, P.O. Box 218, Yorktown Heights, NY 10598; bge@watson.ibm.com.

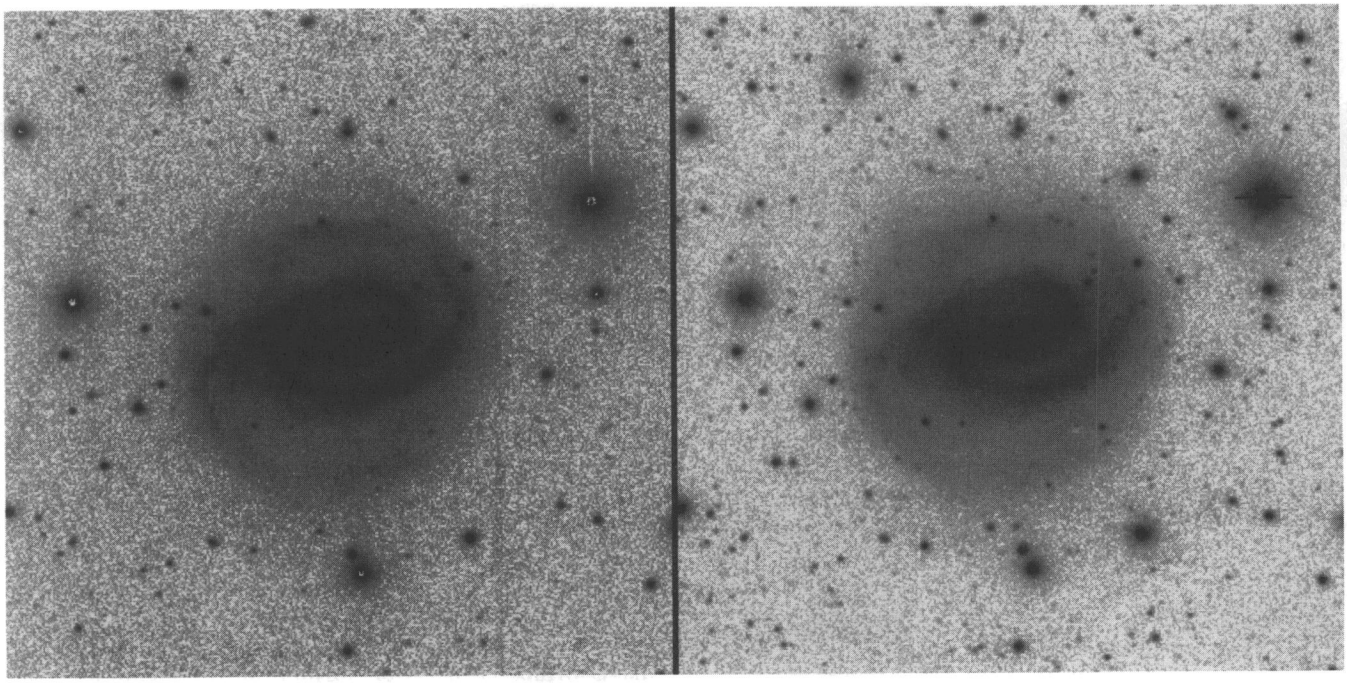

FIG. 1.—*B* (*left*) and *I* (*right*) band sky images of NGC 1300 shown on a logarithmic scale to enhance the outer pseudo-ring

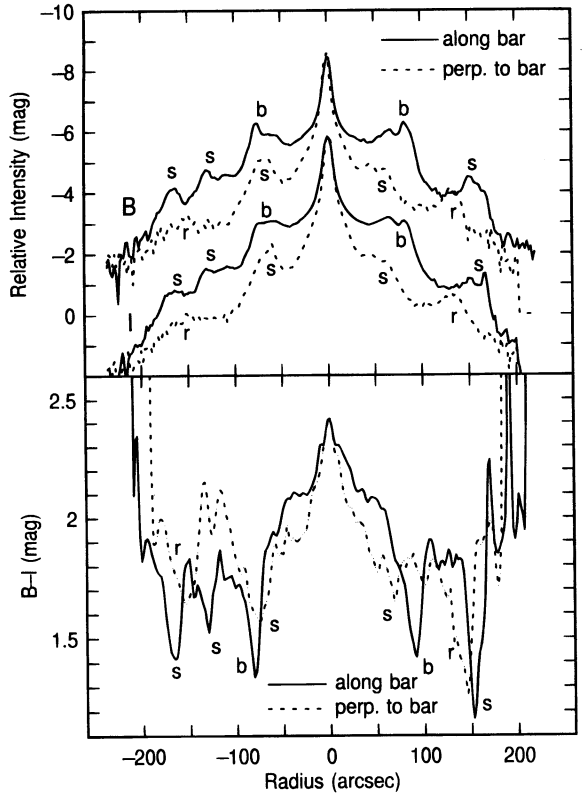

FIG. 2.—(*top panel*) Radial profiles in *B* and *I* measured along the bar (*solid line*) and perpendicular to the bar (*dashed line*). The bar radius is 79″, while the outer ring is 130″ (north, *top*) and 150″ (south) from the center of the galaxy on the perpendicular cut. Features are indicated by "r" (ring), "s" (spiral), and "b" (bar). (*bottom panel*) Radial profiles in $(B-I)$. Relative intensities are plotted in the top panel; the zero point for the *B* intensity corresponds to a surface brightness of 28.25 mag arcsec^{-2}; the zero point in *I* corresponds to 23.55 mag arcsec^{-2}. For the bar-parallel scans, east is to the left; for the perpendicular scans, south is to the left.

prominent in the *B* band than in the *I* band, so the ring colors are blue. The arms are ~1.4 mag brighter in *B* than the interpolation of the interarm regions on each side, and the ring is ~1.1 mag and 1.4 mag brighter than the interpolation from each side in the south and north, respectively. Note that there are no significantly exponential parts in these profiles (as there would be in azimuthally averaged profiles) because the bar is a flat-profile type (Elmegreen & Elmegreen 1985; Elmegreen et al. 1996) and the outer disk is strongly influenced by spiral arms and the outer ring. The slight dip near the center on the $B-I$ plot in the parallel-to-bar direction is from the blue nuclear ring (Pogge 1989).

Photometric calibration was based on observations of M67 (Montgomery, Marschall, & Janes 1993) made during the 1995 run. Standard magnitudes for 56 stars in the field of NGC 1300 were computed from the 1995 frames, and these local standards were in turn used to calibrate our 1994 data. Surface photometry from our calibrated images can be compared with other published results. In particular, we find that the blue isophote at 25 mag arcsec^{-2} is only approximately elliptical in shape, with an isophotal semi-major axis of 3.′15 ± 0.′07 at a position angle of 105° ± 3°. The effective semiminor axis, computed to give the correct area inside a fitted elliptical isophote, is 2.′04 ± 0.′07. The values for the same quantities given in the RC3 are 3.′08 ± 0.′07, 106°, and 2.′03 ± 0.′09, respectively. We correct our measured value of the major axis for Galactic absorption (see RC3) and adopt $R_{25} = 3.'22$ for this paper. We can also compare our digital aperture photometry of NGC 1300 with the available photoelectric measurements. H. Corwin (1995, private communication) found a *B* magnitude of 11.53 and a $B-I$ color of 1.960 inside an aperture of radius 1.′64; for the same aperture we get 11.50 ± 0.02 mag and 1.811 ± 0.03 mag. Corwin also reports R. Smyth observations of a *B* magnitude of 11.57 and a $B-I$ color of 1.855

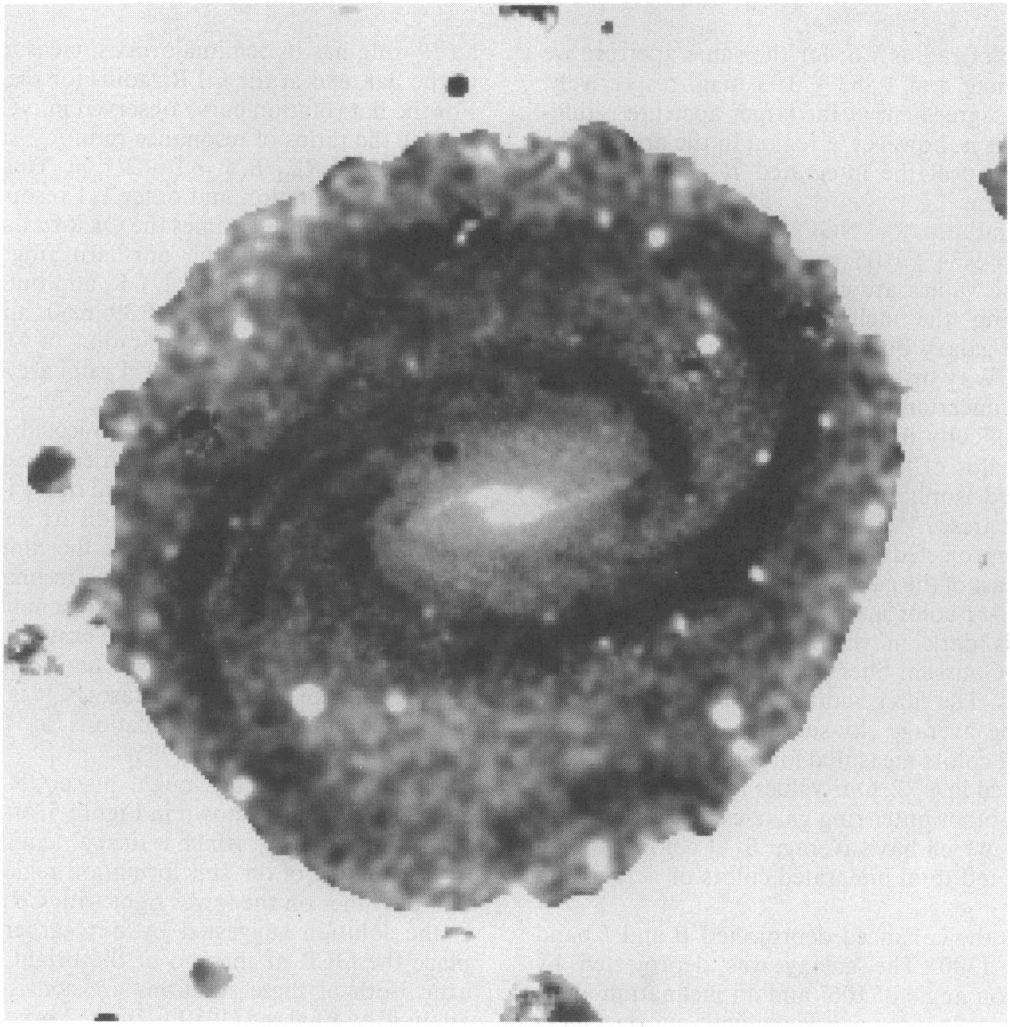

FIG. 3.—$B-I$ color map of NGC 1300, ranging from $B-I = 0.8$–2.5 mag, with the average uncorrected color of the ring equal to 1.4 mag. Sky pixels have been masked, and outer regions were smoothed.

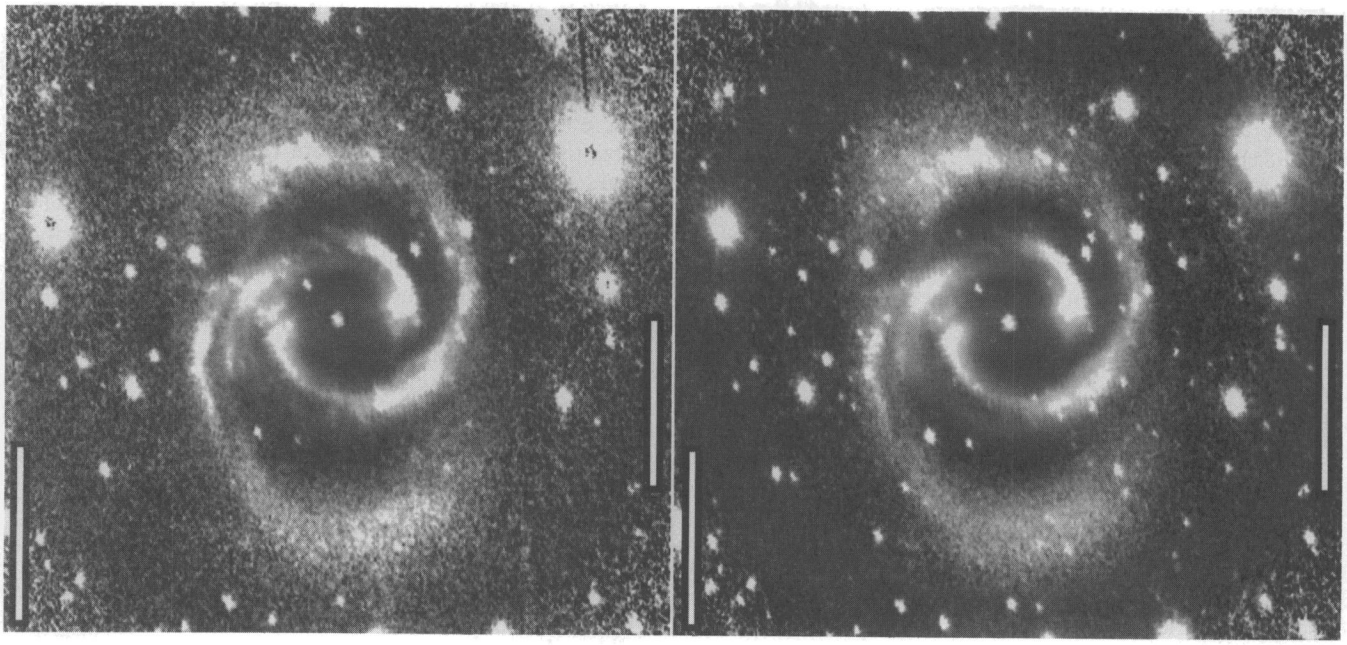

FIG. 4.—Enhanced B (*left*) and I (*right*) band images of NGC 1300. In each figure, the calibration bar on the right indicates R_{25} and the bar on the left indicates 100 pixels.

inside an aperture of radius 1.6; for the same aperture we get 11.57 ± 0.02 mag and 1.853 ± 0.03 mag, respectively. The substantial disagreement at the larger aperture is difficult to explain. This is, however, a region in the arms of the galaxy where we expect the integrated $B-I$ color to be decreasing with radius.

The total magnitudes for NGC 1300 are $B_T = 11.12 \pm 0.04$ mag, $I_T = 9.34 \pm 0.05$ mag, and $(B-I)_T = 1.78 \pm 0.06$ mag. These values are corrected for obvious foreground stars using the stellar point spread function observed near the galaxy but are not corrected for extinction by the Milky Way or by dust in NGC 1300 itself. The greatest source of uncertainty in the integrated magnitudes arises from the difficulty in estimating the contribution of the overlapping halos of foreground stars. The outermost reliably determined isophote in the B image is at surface brightness 27 mag arcsec^{-2}; it is nearly circular in shape on the sky (i.e., not deprojected), with a radius of 3.53, centered 10″ south and 9″ east of the galaxy nucleus.

A calibrated $B - I$ color map of NGC 1300 is shown in Figure 3 (blue is dark in the figure). The image was smoothed with a Gaussian filter applied separately to four concentric regions. The filter width varied inversely as the square root of the average sky-subtracted signal in each annulus. The $B-I$ colors measured for different parts of the galaxy are discussed in § 3.2. Our values are consistent with the color maps of other outer ring galaxies imaged by Buta & Crocker (1991), which have average $B-I$ colors ranging from ~1.5 to 2.5 and total integrated colors of ~1.8 (Buta & Crocker 1992).

Figure 4 shows the enhanced deprojected B and I band images of NGC 1300. The galaxy was deprojected by assuming a position angle of 106° and an inclination angle of 48° (RC3); these values are consistent with our own measurements, discussed above. The enhancement was made by subtracting the azimuthally averaged radial light profile (Elmegreen, Elmegreen, & Montenegro 1992, hereafter EEM). The bar has an inclination-corrected half-length of approximately 79″ (out to the midpoint of the bar-spiral arm transition). This half-length corresponds to $0.41R_{25}$ for a radius at 25th magnitude arcsec^{-2} $R_{25} = 3.23$ from our photometry (which gives $\log R_{25} = 1.81$ instead of the value of 1.79 listed in the RC3), and it corresponds to a half-length of 6.6 kpc for a distance of 17.1 Mpc (de Vaucouleurs & Peters 1981).

3. DISCUSSION

3.1. *Resonances*

The deprojected radii of the central parts of the outer rings in the north and south are 3.3 and 4.0, respectively, from Figure 4. These distances correspond to $1.02R_{25}$ and $1.23R_{25}$, and to 16.4 kpc and 19.9 kpc for 17.1 Mpc galaxy distance. Normally, an R'_1 ring is more symmetric than this, but NGC 1300 has a dwarf elliptical companion galaxy, NGC 1297, 19.6 to the north with a similar velocity (1550 and 1599 km s^{-1} for NGC 1300 and NGC 1297, respectively; Palumbo, Tanzella-Nitti, & Vettolani 1983). The companion could have distorted the ring or the disk plane in NGC 1300 during a recent encounter. No optical bridge between the galaxies is evident though.

We attempt to find the corotation and other resonance radii from morphological features. According to Schwarz (1984), Buta & Crocker (1991, 1993), and Byrd et al. (1994), an R'_1 ring has its semimajor axis, measured perpendicular to the bar, end at the OLR radius for the bar-ring pattern. For the flat rotation curve observed in NGC 1300 (England 1989a), the ratios of resonance radii $R_{m:1}$ to corotation R_{CR} are given by $R_{m:1}/R_{CR} = 1 - 2^{1/2}/m$. This implies that the inner 4:1, corotation and outer 1:1 resonance radii should be 0.38, 0.59, and 1.41 times the OLR radius, respectively.

If the OLR is at the northern ring radius of 3.3 = $1.02\ R_{25}$, then the inner 4:1, CR, and outer 1:1 radii are at 1.3, 1.9, and 4.7, which are 0.39, 0.60, and $1.44R_{25}$. If the OLR is at the southern ring radius of 4.0 = $1.23R_{25}$, then the inner 4:1, CR, and outer 1:1 radii are at 1.5, 2.4, and 5.7, which are 0.47, 0.72, and $1.73R_{25}$. These two possibilities are shown as circles on the deprojected images in the top left and top right of Figure 5. In each case the four circles are at the inner 4:1, CR, OLR, and outer 1:1 radii.

These theoretical resonance radii are sensible if the bar, at $\sim 0.41R_{25}$, ends slightly outside the inner 4:1 resonance, and the spiral begins between this resonance and CR. For the OLR = $1.23R_{25}$ case, the CR resonance corresponds to a point of bifurcation in both the eastern and western arms (see Fig. 5, *top right, second circle out from center*). Considering the average of these two cases, CR is ~1.6 ± 0.1 times the bar radius. Arm bifurcations at CR are common (Elmegreen & Elmegreen 1995).

Other considerations might place CR closer to the bar end. These are also shown in Figure 5, one on the lower left with CR at $0.41R_{25}$, which is the bar length measured above (to the middle of the star formation region at the bar end), and the other on the lower right with CR at $0.52R_{25}$, which is the solution suggested by our earlier study (EEM) to place the OLR at the end of the bright part of the spiral arm. Both of these solutions are consistent with the H I analysis by England (1989b). In the lower left case, the resonance circles in the figure are at 0.26, 0.41, 0.70, and $0.99R_{25}$, and in the lower right case they are at 0.33, 0.52, 0.88, and $1.25R_{25}$.

In the first of these alternate cases, the OLR is at a break or bifurcation in the western arm, and the outer 1:1 resonance is at the northern outer ring. In the second case, the outer 1:1 resonance passes through the southern outer ring, the OLR is at the ends of the prominent arms before the rings begin, and CR passes close to a place in both arms where the arm intensity becomes weak because of dust features that appear to cross from the inner to the outer arm edges.

The identification of an outer 1:1 resonance with an outer ring has not been suggested by numerical simulations so the last two possibilities mentioned above are not conventional. At the outer 1:1 resonance, stars move with their epicycles locked to the bar pattern such that the largest galactocentric separations occur at a fixed phase relative to the bar position angle. If this resonance produces the outer ring in NGC 1300, then the outer extrema of the 1:1 epicyclic orbit would be at the major axis of the ring perpendicular to the bar; the smallest extrema could occur in the spiral arm on the other side of the bar. To make an outer ring on each side of the bar, there would have to be stars from each side with distinct epicyclic motions. The actual 1:1 resonance radius would not be at the ring position but inside of it, possibly between the outer ring and the next inner spiral arm segment.

The best fits to the resonance positions in NGC 1300 seem to be those with CR midway in the spiral arms, at

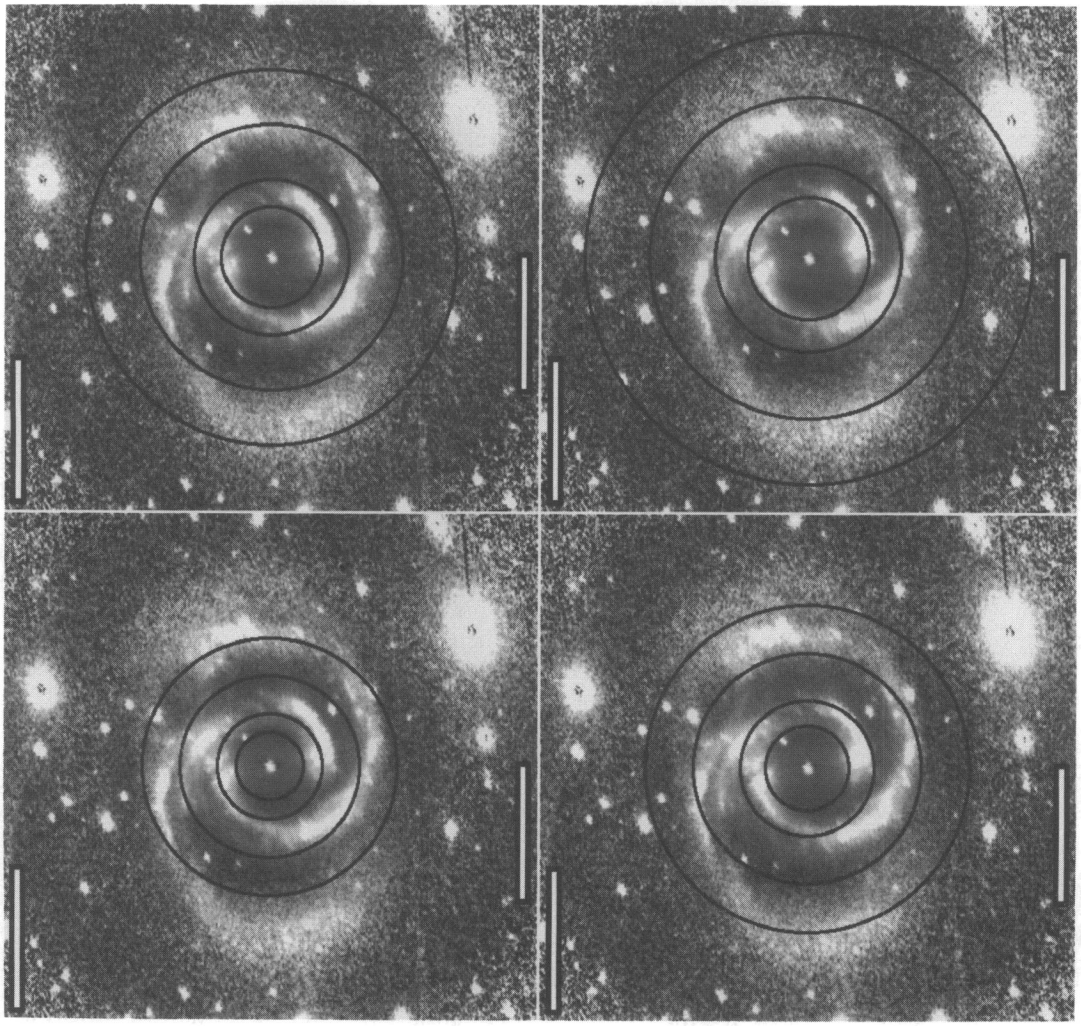

FIG. 5.—Possible resonance locations for NGC 1300. The four circles in each case are possibilities for the inner 4:1 resonance, corotation (CR), outer Lindblad resonance (OLR), and outer 1:1 resonance, assuming a flat rotation curve. The top left panel fits the OLR to the northern radius of the outer ring, giving CR at 1.'9; the top right panel fits the OLR at the southern ring radius, giving CR at 2.'4; the lower left panel fits the end of the bright part of the bar at CR (= 1.'3), and this also puts the northern ring at the outer 1:1 resonance; the lower right panel is from our previous study (EEM, CR = 1.'7), and it places the southern ring radius at the outer 1:1 resonance.

about $1.6 \pm 0.1 R_{\rm bar}$, as shown on the top of Figure 5. These fits place the outer ring at the OLR and corotation at or near the arm bifurcations. The bar then ends between the inner 4:1 and corotation resonances.

3.2. *Ring Color and Age*

The colors of various features were determined in order to estimate ages based on population synthesis models (Leitherer & Heckman 1995). Polar coordinate plots were made of the deprojected B and I images, and azimuthal cuts through these were used for measuring the intensities of the arms, peaks, and interarm regions. In the nucleus, $B-I = 2.4$ mag and in the bar $B-I = 2.2$ mag, uncorrected for extinction.

The intensity of the average ring was determined by subtracting the average background intensity on either side of the ring from the average ring intensity in regions free from obvious star formation peaks. The intensity of a star formation region was determined by subtracting the average ring intensity to the side of the star formation peak from the peak intensity. These excess intensities, from the pure ring and from the pure star formation region, were determined in each passband, and the $B-I$ colors were obtained from the ratios.

Extinction corrections were applied as follows. The foreground extinction from the Milky Way is $A_B = 0.26$ mag (RC3). The average H I column density through the ring is $\sim 6 \times 10^{20}$ cm^{-2}, the average through the star formation regions is $\sim 1 \times 10^{21}$ cm^{-2}, and the average on either side of the ring is $\sim 2 \times 10^{20}$ cm^{-2}, from contours in England (1989a). We convert these column densities to visual extinctions using the factor 2×10^{21} atoms cm^{-2} mag^{-1} (Bohlin, Savage, & Drake 1978) and take half of these extinctions to represent approximate values to the midplane. We also convert visual to B extinctions with $A_B = 1.33 A_V$ and blue to I extinctions with $A_I = 0.4 A_B$. Then the approximate extinctions to the midplane in the star formation peaks, the average ring between the peaks, and the region outside the ring are, in mag, $(A_B, A_I) = (0.33, 0.13)$, (0.2, 0.08), and (0.066, 0.027), respectively, plus the Galactic values of (0.26,

0.10) mag. The corrected intensities in these regions are therefore larger than the observed intensities by the factors ($10^{0.4A_B}$, $10^{0.4A_I}$), which, including Galactic extinction, are (1.72, 1.24), (1.53, 1.18), and (1.35, 1.12) in the three types of regions, respectively. Note that by considering the observed H I column densities, not deprojected to a face-on view, we are automatically including inclination corrections in the extinction.

The colors were determined from the corrected intensities. If I_{bkg} is the mean intensity in the I band of the background disk on either side of the ring and I_{ring} is the intensity from a portion of the ring, and if B_{bkg} and B_{ring} are the corresponding values in the B band, then the ring-only $B-I$ color is $-2.5 \log_{10}([1.53B_{ring} - 1.35B_{bkg}]/[1.18I_{ring} - 1.12I_{bkg}])$.

The $B-I$ colors of the clumpy blue regions in the ring, which we identify with star formation regions (sfr), are similarly determined by subtraction of the background ring light: $-2.5 \log_{10}([1.72B_{sfr} - 1.53B_{ring}]/[1.24I_{sfr} - 1.18I_{ring}])$.

The background-subtracted average ring color corrected for extinction is in the range $B-I = 0.66$ to 1.19 mag (average 0.96 mag), which corresponds to an age range of $10^{7.6}$–$10^{10.3}$ yr, with an average value equal to $10^{9.2}$ yr. These ages were determined with a power-law extrapolation of the continuous evolutionary model with solar metallicity in Leitherer & Heckman (1995). The colors to the side of the ring, in the underlying disk, range from 1.3 to 1.5 mag, with a slight gradient that becomes bluer outward. The corresponding age is $\sim 10^{10}$ yr, but extrapolation to such large values from Leitherer & Heckman (1995) is very uncertain. These results suggest most of the ring stars formed when the disk gas first accumulated in the ring, $\sim 10^9$ yr ago.

The ring-subtracted average color in the star formation regions, corrected for extinction, is in the range $B-I = 0.15$–0.85 mag (average 0.58), corresponding to ages from less than 10^7 yr to $10^{8.6}$ yr, with the average color corresponding to $10^{7.3}$ yr, in the continuous mode. These ages are reasonable for large bright star formation regions similar to the star complexes studied by Efremov (1995). Note that we expect the largest regions to have the longest continuous star formation (Elmegreen & Efremov 1996).

We conclude from this that the blue peaks in the ring are normal bursts of star formation with ages in the range of less than 10^7 to $10^{8.6}$ yr, as given above, and that the ring itself formed most of its stars and gas $\sim 10^9$ yr earlier. The ring is not as old as the whole galaxy; presumably it formed after several revolutions by the gradual expulsion of inner disk material torqued up by the bar. This scenario requires a bar age of at least several $\times 10^9$ yr, possibly equal to that of the oldest part of the disk; i.e., the bar formed soon after the disk formed.

In order to investigate further the star-forming regions in the ring, we compared our optical observations with H I maps. VLA H I contours in work by England (1989a, 1989b) show emission extending beyond the outer ring and a good correspondence between the gas and the stars in the ring. An overlay of the H I contours and the $B-I$ image is in Figure 6 (Plate 1). The outer H I and optical arms curve inward rather than form a complete full circle. The lumpy structure in the southern H I arm mimics the variation in blue intensity and color in the arm. The northern H I structure is less well defined, since it spreads out over the disk, but it still coincides with the outermost optical ring. The optical arms as well as the H I arms can be traced over 300° in azimuth.

We estimate that the H I clumps in the outer ring have column densities of about 1×10^{21} cm^{-2}, based on contours by England (1989a). The corresponding masses contained within the peak regions are about 3×10^8 $M_\odot$. If these clouds continue to evolve by contraction, accretion from the adjacent ring gas, and star formation, then they will become more and more isolated from other ring gas and increasingly similar to dwarf galaxies.

The Q parameter is a measure of the stability of the disk against star formation; a value in excess of unity represents stability (see Kennicutt 1989). It equals $\kappa c/(\pi G\sigma)$ for epicyclic frequency κ, velocity dispersion c, and mass column density σ. To evaluate Q, we use the H I rotation curve and column densities given by England (1989a). The rotation curve is flat in the outer disk, so $\kappa = 2^{1/2}V/R$, with deprojected rotation speed $V = 170$ km s^{-1}, $R = 14.5$ kpc, and $N(\text{H I}) = 6 \times 10^{20}$ cm^{-2} for the outer southeastern H I ring. We assume a disk velocity dispersion of 7 km s^{-1}, which is typical for spiral galaxies (Dickey, Hanson, & Helou 1990). Then $Q \sim 1.4$ in the southeast part of the outer ring. In contrast, the regions just inside and outside the outer ring have column densities of 2.5 and 2.2×10^{20} cm^{-2}, based on England's Figure 5, so Q at these radii is 3.3 and 3.7, respectively. The lower value of Q in the outer ring suggests that the ring is blue because of locally enhanced star formation at close to the threshold column density (which has $Q \sim 1.4$; see Kennicutt 1989). The regions immediately interior to the ring and exterior to the ring are stable against star formation.

The timescale for star formation is about $1/\kappa$ (Elmegreen 1994), so the above values give $\sim 6 \times 10^7$ yr. The inferred ages of the clumps are therefore consistent with the interpretation that the star formation is the result of a parallel instability in the ring. This is essentially the same star formation process as described for nuclear resonance rings in Elmegreen (1994), but here it is at a much lower threshold density because of the lower value of κ in the outer disk. Presumably, such instabilities have occurred more or less continuously in the outer ring as it accumulated gas swept out from the disk. Note that the agreement between the instability age and the star formation age in this model rules out the possibility that a dynamically significant amount of cold undetected gas is in the outer disk (Elmegreen 1996).

4. CONCLUSIONS

NGC 1300 has an outer gaseous pseudo-ring of the type R' (Buta & Crocker 1991) that is usually assumed to lie at the OLR in a barred galaxy (Schwarz 1984; Byrd et al. 1994). It also has an outer stellar ring at the same location that is slightly bluer than the background disk. Clumps in the ring are bluer yet, and are probably local star formation. The extinction-corrected $B-I$ colors of the ring and clumps, after removing the underlying disk and the average ring intensity, respectively, give a ring age of $\sim 10^9$ yr and clump ages of several $\times 10^7$ yr. The clumps occur in $10^{8.5}$ $M_\odot$ H I clouds that are probably the result of gravitational instabilities along the length of the ring.

The outer ring radius can be used to estimate the position of corotation for the bar-ring pattern. Our best solution places the end of the bar between the inner 4:1 resonance and corotation, and it suggests there is a sharp bifurcation

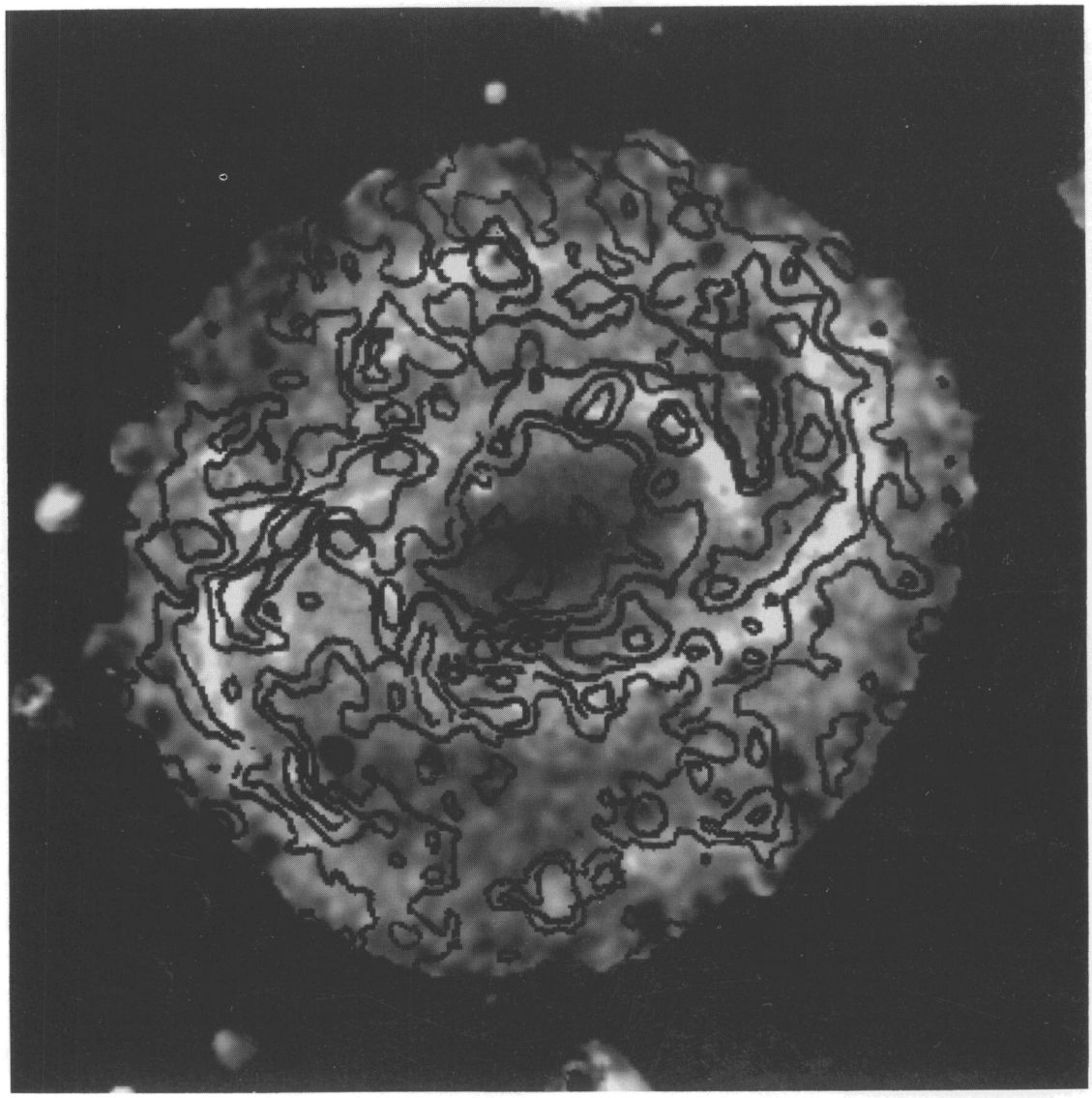

FIG. 6.—H I contours from England's (1989a) VLA data are superposed on the $B-I$ color sky image from Fig. 3. Notice that many H I clumps in the outer ring correspond to blue optical features, indicative of star formation.

in the spiral arms at corotation. The outer ring has its major axis 70° offset from the bar and at a position close to the outer Lindblad resonance. Because of these close alignments between optical features and likely associated resonances, and because of the elongation of the ring nearly perpendicular to the bar, the bar, spiral, and ring patterns all appear to rotate with about the same angular speed. If the perpendicular alignment of the ring is merely coincidental, then the bar, spiral, and ring patterns could be coupled at resonances other than corotation.

D. M. E. and B. G. E. gratefully acknowledge support from the National Science Foundation through grant AST 92-01640. D. M. E., F. R. C., and D. A. H. gratefully acknowledge support from the Wm. Keck Foundation to the Keck Northeast Astronomy Consortium, and D. M. E. from an AAS Small Research Grant for the completion of the project. Observations were obtained at the Burrell Schmidt, which is owned by Warner and Swasey Observatory, Case Western Reserve University, under the auspices of the NorthEast Schmidt Telescope Astronomy Consortium (NESTAC). Helpful comments by R. Buta are appreciated. We are grateful to Harold Corwin for communication of photoelectric data, and to J. Trent Adams and C. Olivia Johnson for assistance obtaining the 1994 and 1995 observations, respectively.

REFERENCES

Baumgart, C. W., & Peterson, C. J. 1986, PASP, 98, 56
Bohlin, R. C., Savage, B. D., & Drake, J. F. 1978, ApJ, 224, 132
Buta, R. 1995, ApJS, 96, 39
Buta, R., & Crocker, D. 1991, AJ, 102, 1715
———. 1992, AJ, 103, 1804
———. 1993, AJ, 105, 1344
Byrd, G., Rautiainen, P., Salo, H., Buta, R., & Crocker, D. A. 1994, AJ, 108, 476
de Vaucouleurs, G., & Buta, R. 1980, AJ, 85, 637
de Vaucouleurs, G., & Peters, W. L. 1981, ApJ, 248, 395
de Vaucouleurs, G., de Vaucouleurs, A., Corwin, H. G., Jr., Buta, R., Paturel, G., & Fouque, P. 1991, Third Reference Catalogue of Bright Galaxies, (New York: Springer) (RC3)
Dickey, J. M., Hanson, M. M., & Helou, G. 1990, ApJ, 352, 522
Efremov, Yu. N. 1995, AJ, 110, 2757
Elmegreen, B. G. 1994, ApJ, 425, L73
———. 1996, in Cold Dust and Galaxy Morphology, ed. D. Block (Dordrecht: Kluwer), in press
Elmegreen, B. G., & Efremov, Yu. N. 1996, ApJ, 467, in press
Elmegreen, B. G., & Elmegreen, D. M. 1985, ApJ, 288, 438
Elmegreen, B. G., Elmegreen, D. M., Chromey, F. R., & Hasselbacher, D. A. & Bissell, B. A. 1996, AJ, 111, 1880
Elmegreen, B. G., Elmegreen, D. M., & Montenegro, L. 1992, ApJS, 79, 37 (EEM)
Elmegreen, D. M., & Elmegreen, B. G. 1995, ApJ, 445, 591
England, M. N. 1989a, ApJ, 337, 191
———. 1989b, ApJ, 344, 669
Kennicutt, R. C. 1989, ApJ, 344, 685
Leitherer, C., & Heckman, T. 1995, ApJS, 96, 9
Montgomery, K. A., Marschall, L. A., & Janes, K. A. 1993, AJ, 106, 181
Palumbo, G. G. C., Tanzella-Nitti, G., & Vettolani, G. 1983, Catalogue of Radial Velocities of Galaxies (New York: Gordon & Breach)
Pogge, R. W. 1989, ApJS, 71, 433
Schwarz, M. P. 1981, ApJ, 247, 77
———. 1984, MNRAS, 209, 93